

This article was downloaded by:

On: 25 January 2011

Access details: *Access Details: Free Access*

Publisher *Taylor & Francis*

Informa Ltd Registered in England and Wales Registered Number: 1072954 Registered office: Mortimer House, 37-41 Mortimer Street, London W1T 3JH, UK



Liquid Crystals

Publication details, including instructions for authors and subscription information:

<http://www.informaworld.com/smpp/title~content=t713926090>

Mesomorphic and dielectric properties of fluorosubstituted isothiocyanates with different bridging groups

Joanna Czub^a; Roman Dąbrowski^b; Jerzy Dziaduszek^b; Stanisław Urban^a

^a Institute of Physics, Jagiellonian University, Reymonta 4, Krakow, Poland ^b Institute of Chemistry, Military University of Technology, Kaliskiego 2, Warsaw, Poland

Online publication date: 05 November 2010

To cite this Article Czub, Joanna , Dąbrowski, Roman , Dziaduszek, Jerzy and Urban, Stanisław(2009) 'Mesomorphic and dielectric properties of fluorosubstituted isothiocyanates with different bridging groups', *Liquid Crystals*, 36: 5, 521 – 529

To link to this Article: DOI: 10.1080/02678290903039125

URL: <http://dx.doi.org/10.1080/02678290903039125>

PLEASE SCROLL DOWN FOR ARTICLE

Full terms and conditions of use: <http://www.informaworld.com/terms-and-conditions-of-access.pdf>

This article may be used for research, teaching and private study purposes. Any substantial or systematic reproduction, re-distribution, re-selling, loan or sub-licensing, systematic supply or distribution in any form to anyone is expressly forbidden.

The publisher does not give any warranty express or implied or make any representation that the contents will be complete or accurate or up to date. The accuracy of any instructions, formulae and drug doses should be independently verified with primary sources. The publisher shall not be liable for any loss, actions, claims, proceedings, demand or costs or damages whatsoever or howsoever caused arising directly or indirectly in connection with or arising out of the use of this material.

Mesomorphic and dielectric properties of fluorosubstituted isothiocyanates with different bridging groups

Joanna Czub^{a*}, Roman Dąbrowski^b, Jerzy Dziaduszek^b and Stanisław Urban^a

^a*Institute of Physics, Jagiellonian University, Reymonta 4, 30-059 Krakow, Poland;* ^b*Institute of Chemistry, Military University of Technology, Kaliskiego 2, 00-908 Warsaw, Poland*

(Received 13 March 2009; final form 12 May 2009)

Results of the phase transition and the static and dynamic dielectric investigations of several new liquid crystalline compounds, consisting of three phenyl rings with the alkyl and isothiocyanato terminals, fluoro lateral substituents, and different bridging groups, are presented. These compounds form the nematic phase accompanied in some cases by a smectic phase. The dielectric parameters are analysed in relation to the dipole structures of the molecules. In the nematic phase some compounds with a bridging carboxylic group exhibit the crossover of the principal permittivity components within the megahertz frequency range.

Keywords: liquid crystals; nematic phase; dielectric permittivity; dipole structure

1. Introduction

Dielectric studies of liquid crystals (LCs) yield important information on molecular reorientations and their interactions in mesophases. Knowledge of the dielectric properties of LCs is also important for technical reasons, due to their application in electro-optical display devices. The aim of the present work was to analyse the influence of different substituents and bridging groups on the dielectric properties of selected isothiocyanates. The chemical structures of the compounds studied are shown in Table 1. Most of the investigated compounds are enantiotropic nematogens in a broad temperature range, except compounds **4** and **9**. The former exhibits the monotropic nematic (N) phase appearing in a narrow temperature range during cooling, whereas the latter does not exhibit a LC phase. The common features of dielectrically studied substances are three phenyl rings and the same terminal groups ($-\text{C}_4\text{H}_9$ and $-\text{NCS}$). However, due to various bridging groups (CH_2CH_2 and/or COO) and fluorine atom(s) at different lateral positions, their dipole structures are differentiated. All of them possess strong longitudinal and moderate transverse dipole components. This should be reflected in the dielectric properties of the N phase observed at low frequencies (a static case), as well as at high frequencies (a dynamical case). One of the aims of the work was to find a relation between molecular structure and crossover frequencies. The high birefringence compounds changing the sign of dielectric

anisotropy are especially interesting, because they enable one to accelerate the LC dynamics (1–4). In addition, the dielectric properties of LC materials in the high frequency region are now becoming objects of increasing interest (5).

2. Experimental

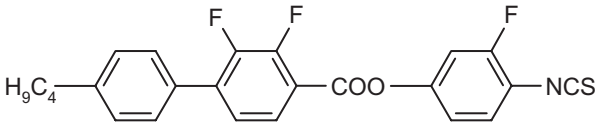
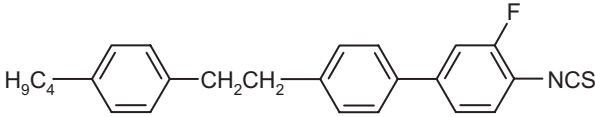
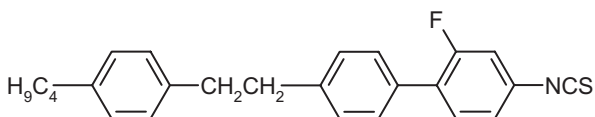
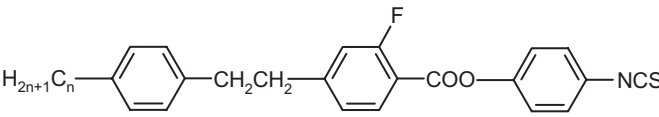
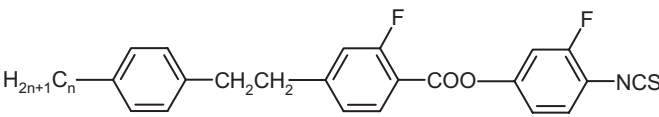
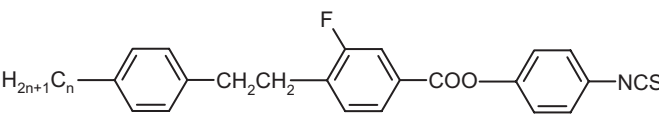
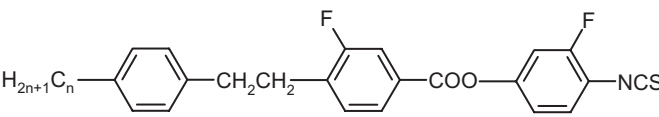
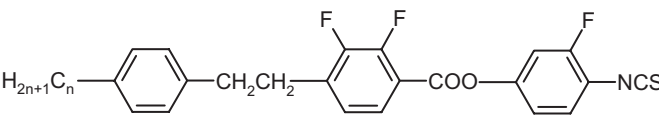
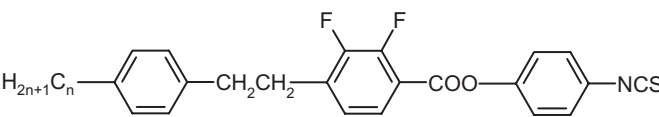
All substances were synthesised in the Institute of Chemistry, Military University of Technology, Warsaw. The preparation of compound **1** is described in (4), compounds **2** and **3** in (6) and the synthetic routes to compounds **4–9** are shown in Scheme 1.

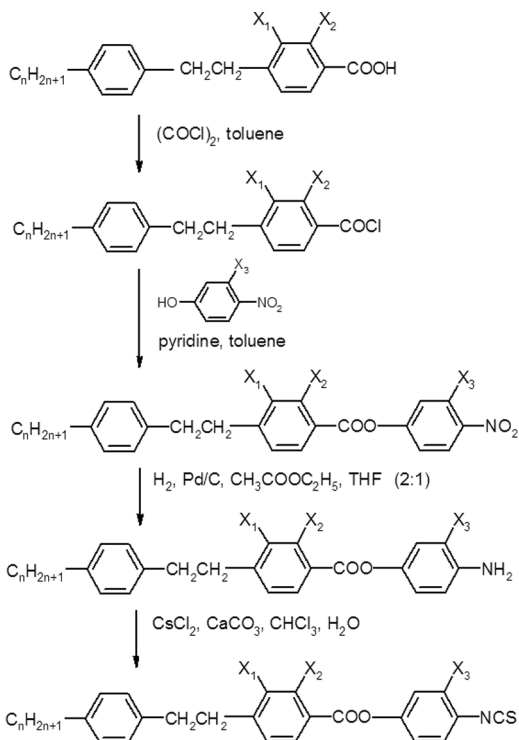
At the first stage nitroesters (see Scheme 1) were synthesised from commercial 4-nitrophenol or 3-fluoro-4-nitrophenol (Aldrich) and 4-(4-alkylphenylethyl-2)-2-fluorobenzoic acids or 4-(4-alkylphenylethyl-2)-3-benzoic acids according to the multistage procedure presented in Schemes 2 and 3, respectively. The 4-(4-alkylphenylethyl-2)-2,3-difluorobenzoic acids were prepared similarly to the 4-(4-ethylphenylethyl-2)-2-difluorobenzoic acids (Scheme 3), but with the difference that 2,3-difluorotoluene was the first substrate and $\text{C}_4\text{H}_9\text{Li}$ was used for lithiation in the last stage. Then, nitroesters were reduced to aminoesters by hydrogen in the presence of a palladium catalyst on carbon and the aminoesters were treated with thiophosgene. The preparation conditions of all these synthetic steps were the same as described in (7).

The phase transition temperatures (onset point) and melting enthalpies were measured with a

*Corresponding author. Email: joanna.czub@uj.edu.pl

Table 1. Chemical structures, phase transition temperatures and melting enthalpy (from differential scanning calorimetry measurements, onset point, °C and kJ mol⁻¹, respectively) of the compounds studied.

Acronym	Chemical structure
1	 <p>Cr 71.6 SmA 158.5 N 195.7 I [4]</p>
2	 <p>Cr 57.7 N 111.8 I; ΔH=24.4 [6]</p>
3	 <p>Cr₁40.9 Cr₂ 46.4 N 85.2 I [5]; ΔH₁=14.4; ΔH₂=7.95 [6]</p>
4	 <p>n=3 Cr 119.5 N 126 I; ΔH=29.9 n=4 Cr 120.3 (N 116.3) I, ΔH=33.4</p>
5	 <p>n=3 Cr 85.1 N 115.3 I; ΔH=35.7 n=4 Cr₁ 52.9 Cr₂ 73.6 N 104.7 I; ΔH₁=10.2; ΔH₂=22.9</p>
6	 <p>n=3 Cr 115.0 N 122.1 I; ΔH=39.5 n=4 Cr 95.4 N 112.5 I; ΔH=28.9</p>
7	 <p>n=3 Cr 63 N 111.7 I; ΔH=31.5 n=4 Cr 56.9 N 101.3 I; ΔH=31.9</p>
8	 <p>n=4 Cr 91.9 N 102 I; ΔH=28.9</p>
9	 <p>n=4 Cr 132.2 I; ΔH=38.7</p>

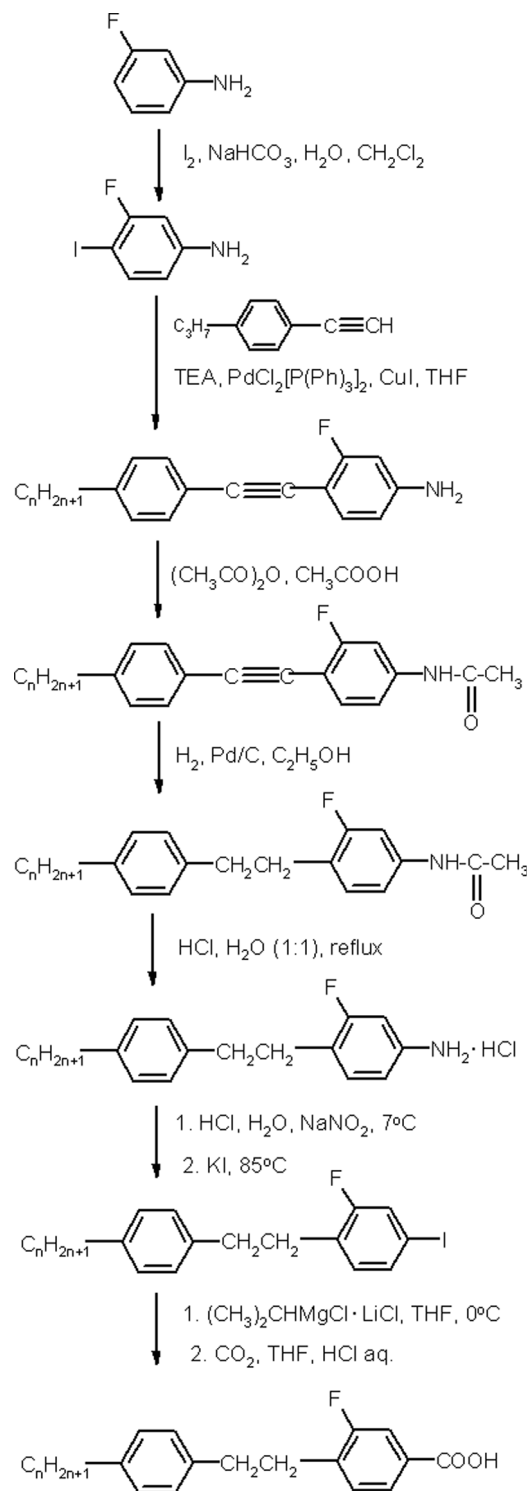


Scheme 1. Synthetic route to fluorinated ester of series 4–7. Compound 4 $X_1 = \text{H}$; $X_2 = \text{F}$; $X_3 = \text{H}$, compound 5 $X_1 = \text{H}$; $X_2 = \text{F}$; $X_3 = \text{F}$, compound 6 $X_1 = \text{F}$; $X_2 = \text{H}$; $X_3 = \text{H}$, compound 7 $X_1 = \text{F}$; $X_2 = \text{H}$; $X_3 = \text{F}$.

SETARAM DSC141 microcalorimeter during the heating cycle, with a heating rate of 2 degrees/min.

The LC phases were identified by observation of their specific patterns under a polarising microscope OLYMPUS BX51 equipped with a heating stage LINKAM THMS600.

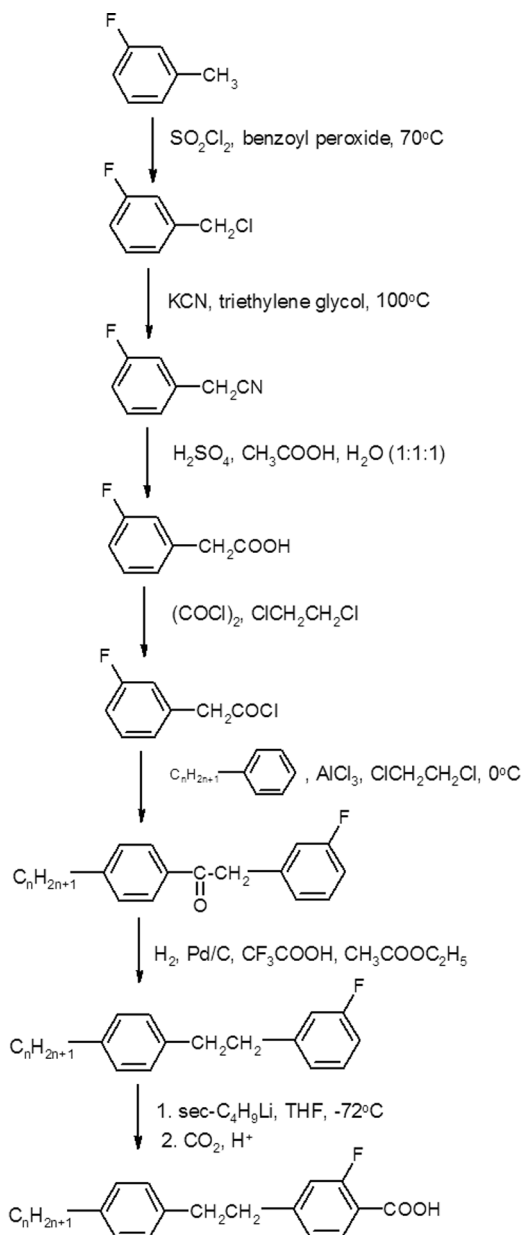
The dielectric relaxation spectra, $\varepsilon^*(f) = \varepsilon'(f) - i\varepsilon''(f)$, were recorded with the aid of an impedance analyser HP 4192A in the frequency range 1 kHz–30 MHz. A parallel plate capacitor was used ($C_o \sim 50$ pF). The thickness of the samples was 0.7 mm and the samples in the N phase were oriented by a magnetic field of 0.8 T. Two experimental geometries were applied, $\mathbf{E} \parallel \mathbf{B}$ and $\mathbf{E} \perp \mathbf{B}$, enabling the measurement of the ε_{\parallel} and ε_{\perp} permittivity tensor components, respectively. The temperature was stabilised within ± 0.1 K in the range 20–90°C and ± 0.2 K in the range 90–160°C. In the isotropic phase a time domain spectrometer (TDS) was employed to cover the frequency range from 10 MHz to 3 GHz (8). All measurements were carried out with decreasing temperature, which caused supercooling of the LC phases. In compounds 5 and 6, a monotropic phase (B or E) was observed during dielectric measurement at room temperature.



Scheme 2. Synthetic route of 4-(4-alkyl-phenylethyl)-2-3-fluorobenzoic acids $n = 3$ or 4.

3. Results and discussion

Figure 1 presents comparisons of the tensor permittivity components, ε_{\parallel} and ε_{\perp} , obtained for the butyl compounds studied. The use of the shifted



Scheme 3. Synthetic route of 4-(4-alkylphenylethyl)-2-fluorobenzoic acid.

temperature scale, $T_{NI} - T$, clearly shows a large scatter of the permittivity values taken at the same distance to the clearing point. Some parameters characterising the dielectric properties of compounds under study are presented in Table 2. At low frequencies all compounds have positive dielectric anisotropy, $\Delta\varepsilon = \varepsilon_{\parallel} - \varepsilon_{\perp} > 0$. However, due to a pronounced dispersion of the parallel component of the permittivity $\varepsilon'_{\parallel}(f)$ occurring at MHz frequencies while the perpendicular component is almost

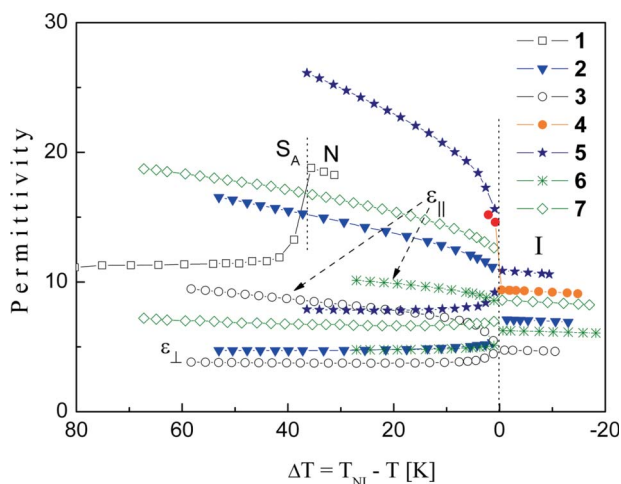


Figure 1. Tensor permittivity components for all substances studied versus shifted temperature.

constant over those frequencies, the anisotropy changes its sign in some cases: in the high frequency region ε_{\parallel} becomes equal to ε_{\perp} or lower. The occurrence of the crossover effect basically depends on the value of the perpendicular component of the dipole moment. If only one F atom is attached at a lateral position (compounds **2** and **3**), the perpendicular permittivity is close to the high frequency permittivity $\varepsilon_{\infty\parallel}$ (Figures 2(a) and (b)), the carbonyl COO bridging group slightly enlarges the ε_{\perp} values and the crossover effect occurs (compound **6**, Figure 2(e)). Certainly, the compounds having two F atoms and the COO bridging group are more effective in that respect – see Figures 2(c) and (d).

The values of the crossover frequency f_{co} are given in Table 2. They are higher than those observed for cyanoesters (**3**). Figure 3 shows that f_{co} strongly depends on the temperature.

Figure 4 shows the structures of the molecules **5** and **6** simulated with the aid of HyperChemTM Release 7.51 and CS Chem3D Pro with CS MOPAC ProTM, based on the semi-empirical AM1 method (9). This software enabled us to calculate the dipole moment components (gathered in Table 2) in order to determine the principal inertia moments axes (marked as 1, 2, 3 in Figure 4) and to estimate the angle β_{cal} between the net dipole moment and the long molecular axis (the 1-axis), as well as the angle β_{chem} between the net dipole moment and the x -axis, defined as the *para*-axis of the middle phenyl ring. As one can see from Figure 4, the *para*-axis differs from the 1-axis by the angle $\Delta\beta$.

Table 2. Quantities determined from the analyses of the results of dielectric measurements: ε_{Is} – the isotropic phase close to T_{NI} ; $\Delta\varepsilon = \varepsilon_{\parallel} - \varepsilon_{\perp}$ taken close to the melting point; μ – dipole moment calculated as explained in the text; β_{Oms} , β_{cat} – angles formed by the dipole moment with the long molecular axis; ΔH_{lf} – activation enthalpy for the low frequency relaxation process in LC phases; f_{co} – the crossover frequency at $T \sim T_{melting}$; $\Delta\varepsilon_{hf}$ – dielectric anisotropy at high frequency.

Substance	μ [D]	β_{cat} [°]	β_{Oms} [°]	ε_I	ε_{\parallel}	ε_{\perp}	$\Delta\varepsilon$	ΔH_{lf} [kJ mol ⁻¹]	f_{co} [MHz]	$\Delta\varepsilon_{hf}$
1	6.38	41.4	–	–	–	–	–	88 (S _A)	–	–
2	3.25	25.2	26.1	7.10	16.54	4.73	11.81	53	–	–
3	1.84	32.3	31.0	4.75	8.39	3.74	4.65	55 (N), 69 (Sm)	–	–
4	5.53	24.1	–	9.39	–	–	–	–	–	–
5	6.38	29.5	25.3	10.86	25.22	7.85	17.37	67	2.86	-2.05
6	3.94	32.0	–	6.26	9.86	4.78	5.08	71.5	5.6	-0.83
7	4.86	36.2	31.9	8.60	17.54	6.85	10.89	62	0.77	-1.68

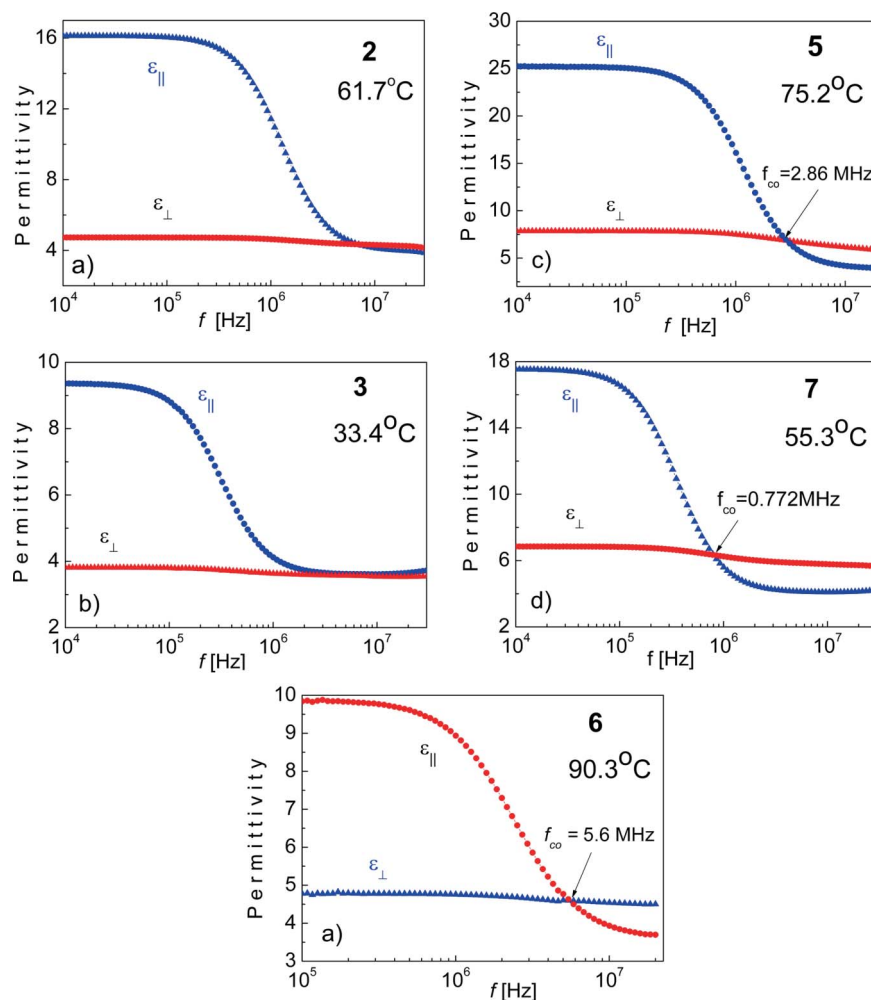


Figure 2. Dispersion spectra collected for compounds **2** and **3** having one F atom without carboxylic group (a), (b), for compounds **5** and **7** having two F atoms and a carboxylic rigid group (c), (d), and compound **6** having one F atom and a carboxylic group giving raise of components μ_l and μ_r of the dipole moment (e). (Small dispersion observed for $\varepsilon_{\perp}(f)$, in particular for **5** and **7**, is connected with the lf relaxation process, because of the order parameter $S < 1$.)

In Table 2, the calculated dipole moment μ for particular substances, together with the angle β_{cat} formed by the dipole moment with the long molecular axis, are listed. The angle β can also be estimated

on the basis of the relaxation spectra in the isotropic phase. Figure 5 shows the TDS spectra collected for two substances in the form of Cole–Cole plots. Superposition of two Debye-type processes,

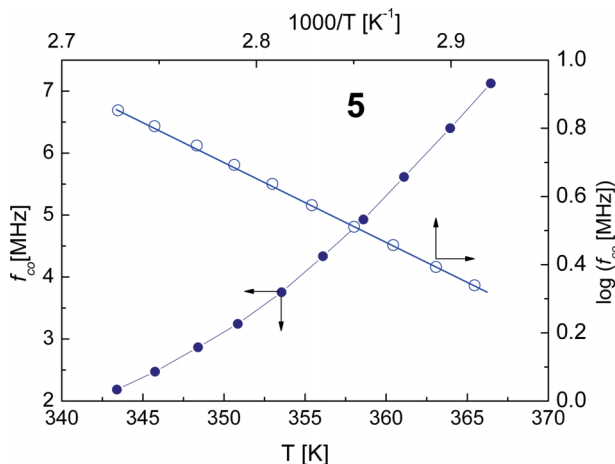


Figure 3. Temperature dependence of the crossover frequency for the N phase of **5**. The $\log f_{co}$ versus $1/T$ plot shows the exponential form of the dependence.

$$\varepsilon^*(\omega) = \varepsilon' - i\varepsilon'' = \frac{\varepsilon_{s1} - \varepsilon_{\infty 1}}{1 + i\omega\tau_1} + \frac{\varepsilon_{s2} - \varepsilon_{\infty 2}}{1 + i\omega\tau_2}, \quad (1)$$

can be fitted to the points that give the ε_s and ε_{∞} values for particular processes (ε_s and ε_{∞} stand for the static and high frequency permittivities, respectively).

By applying the Onsager equation (10),

$$\frac{(\varepsilon_s - \varepsilon_{\infty})(2\varepsilon_s + \varepsilon_{\infty})}{\varepsilon_s(\varepsilon_{\infty} + 2)^2} = \frac{N_0 \mu^2}{3\varepsilon_0 3kT}, \quad (2)$$

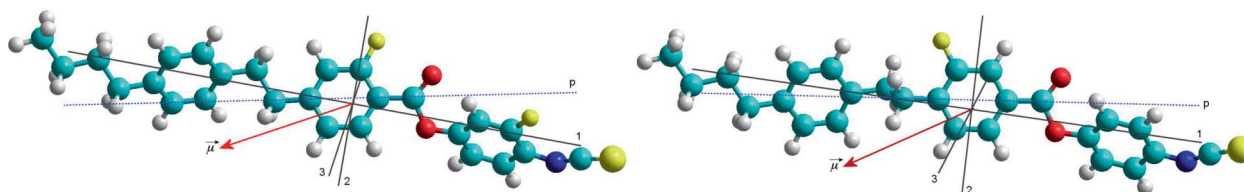


Figure 4. (Colour online). The structure of the **5** (left) and **6** (right) molecules obtained with the aid of the HyperChemTM Release 7.51 program. The inertia moment axes are marked by **1**, **2** and **3**. **p** is the *para*-axis of the middle phenyl ring.

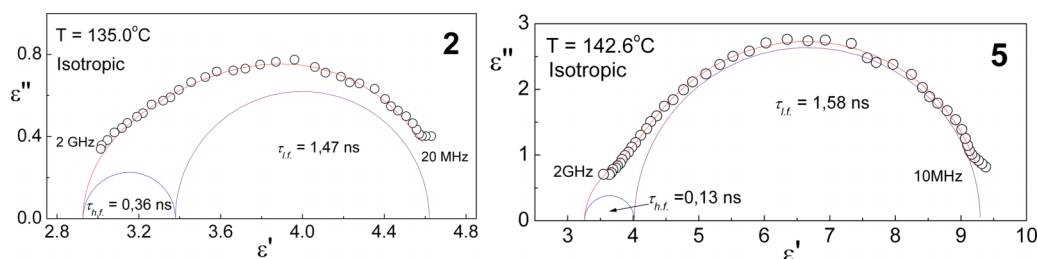


Figure 5. Cole–Cole plots for compounds **2** and **5** in the isotropic phase. The semicircles correspond to two relaxation processes connected with the molecular reorientations about the principal inertia axes. The rotations around the short axes are hindered by the barrier of ca. 37 kJ mol⁻¹, whereas the rotations around the long axes are hindered by ca. 17 kJ mol⁻¹.

separately to the low frequency increment, $\varepsilon_s - \varepsilon_{\infty}$, governed by the longitudinal component μ_l , and to the high frequency increment, governed by the transverse component μ_t , one can calculate the angle $\beta_{Ons} = \tan^{-1}(\mu_t/\mu_l)$. The obtained β_{Ons} values are in reasonable agreement with the β_{cal} ones.

In the N phase, the low frequency relaxation process connected with the molecular rotations about the short axis dominate the spectra for the parallel oriented samples – see Figure 6(a); the same concerns the smectic A phase of **1** – see Figure 6(b). In the monotropic smectic phase observed at low temperatures of **3**, the spectra exhibit a small increment, $\varepsilon_s - \varepsilon_{\infty}$, and a distribution of the relaxation times (the centre of the semicircle is lowered with respect to the ε' axis). The substance in this phase had a consistency typical for crystal-like phases B or E (for example, large plasticity) and remained stable for 24 h at room temperature. After heating, the substance transformed to the N phase. Figure 7 presents the Arrhenius plots for the relaxation times determined for all LC phases. In the reduced scale ($1/T - 1/T_N$), all values of τ are fairly close. The calculated activation enthalpy values, $\Delta H_{||} = R\partial \ln \tau / \partial (T^{-1})$, where R is the gas constant, are listed in Table 2. In spite of the elongated molecular cores, which consisted of three rings with bridging groups, the barriers hindering this voluminous motion seem to be relatively low. Taking into account the very small dielectric increment in the smectic phase of **3**, $\varepsilon_s - \varepsilon_{\infty} \sim 0.1$, and the relatively

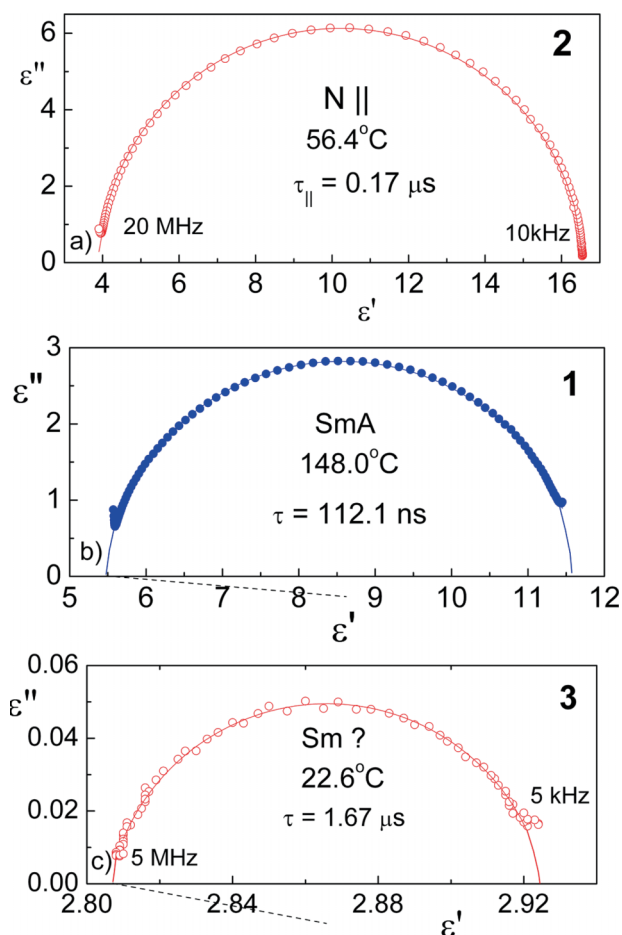


Figure 6. Examples of the Cole–Cole plots for the low frequency relaxation process in LC phases of three compounds.

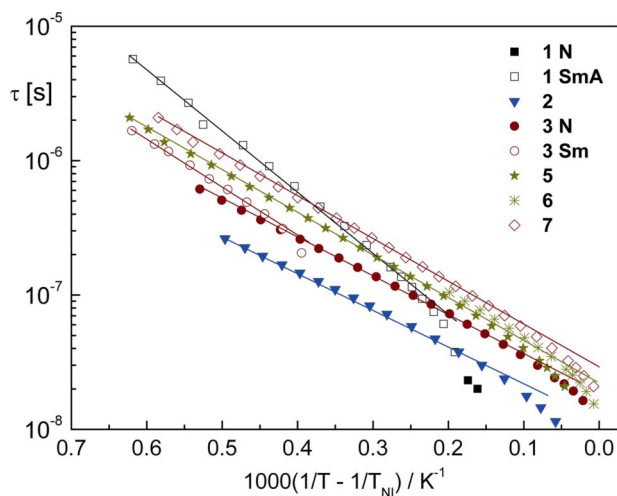


Figure 7. Arrhenius plots for the low frequency relaxation time in the N phase of five substances. On the abscissa axis the scale reduced to the clearing point is used.

short relaxation time at low temperatures ($\sim 1.6 \mu\text{s}$), one can suppose that the observed relaxation process is connected with the molecular rotations around the long axis rather than above the short axis. In the isotropic phase of **5**, the activation barrier for the low frequency relaxation process is equal to 35 kJ mol^{-1} , the value typical for many other LC substances (see, for example, (11, 12)).

It is interesting to compare the dielectric parameters of substances that differ by alkyl chain length. Figure 8 presents the permittivity values for the propyl and butyl members of three homologous series (results for substances with the propyl and NCS terminals will be published separately (13)). Systematically, the ε_{\parallel} component is larger for the shorter member, whereas the calculated dipole moments are practically equal. This feature can be attributed to the odd–even effect originated from the variation with n of the order parameter and is pronounced for short members of a homologous series (14). According to the Maier and Meier equations (15), the dielectric anisotropy is proportional to the order parameter divided by temperature: $\Delta\varepsilon \sim S(T)/T$ (other factors are only slightly dependent upon T). It has been shown that the S -values obtained in this way agree well with those determined by the nuclear magnetic resonance (NMR) and optical anisotropy methods (16, 17). The order parameters calculated in this way are presented in Figure 9.

Figure 10 shows that the low frequency relaxation times and the activation barrier that hinder the flip-flop molecular motions are not sensitive to the change of the alkyl tail length.

4. Conclusions

The substances consisting of three phenyl rings, having the same terminal substituents but different bridging groups and lateral substituents, allowed us to search for the relationships between the structure of molecules and phase transition and the dielectric (static and dynamic) properties of compounds in LC phases. The presence of a fluorosubstituted ethane (CH_2CH_2) bridge in molecules of the investigated compounds involves stronger decrease of the melting points than clearing points (compounds **2** and **3**) and, therefore, the N phase is observed in a large range and also in a supercooled state down to room temperature.

This is not fulfilled in the case of compounds having simultaneously $-\text{CH}_2\text{CH}_2-$ and $-\text{COO}$ bridges, in particular for mono- and difluorosubstituted compounds in the central ring (compounds **6**, **8** and **9**).

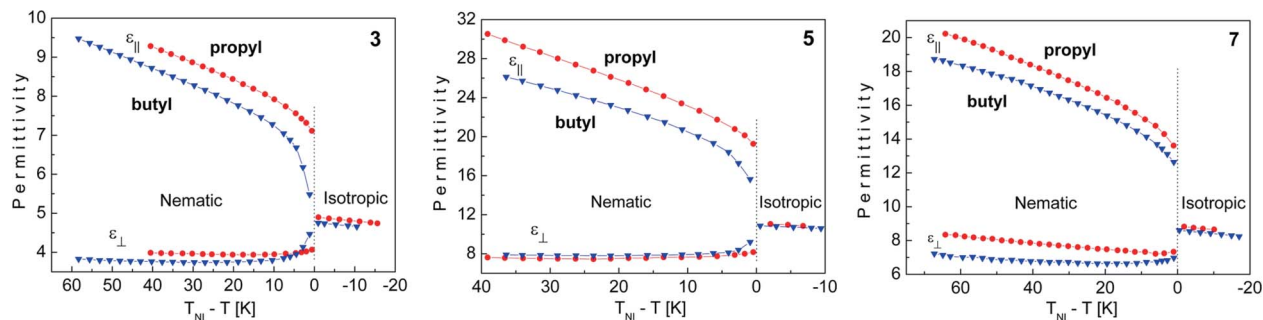


Figure 8. Comparison of the permittivity values measured for the propyl and butyl members of three homologous series.

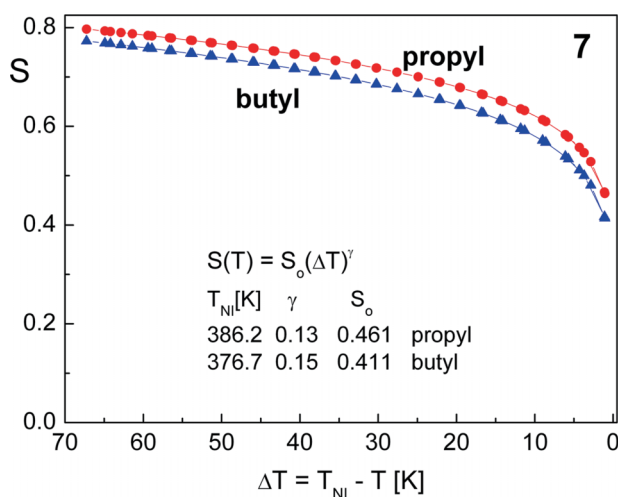


Figure 9. Order parameter calculated from the dielectric increments for two substances. The Haller-type formula with parameters shown in the inset describes the data very well.

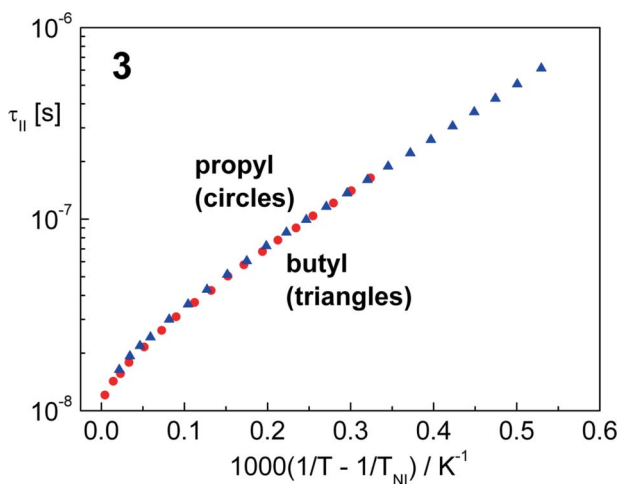


Figure 10. Comparison of the longitudinal relaxation time for the propyl and butyl members of one homologous series.

This is an unexpected result, because usually compounds fluorosubstituted in the central ring have the lowest melting points. The presence of the polar COO group and the flexible CH₂CH₂ bridge probably lead to stronger packing of molecules in the solid phase, which is confirmed by high melting enthalpy, as well as high melting points. It was shown that nematogens with one or two F atoms at the lateral positions, combined with the carboxyl bridging group, lead to the appearance of a crossover in the frequency dependence of the dielectric anisotropy.

Acknowledgement

The synthetic part of this work was supported by the Polish Ministry of Sciences and Higher Education, Key Project POIG.01.03.01-14-016/08, 'New Photonic Materials and their Advanced Applications'.

References

- (1) Xianyu, H.; Zhao, Y.; Gauza, S.; Liang, X.; Wu, S.-T. *Liq. Cryst.* **2008**, *35*, 1129–1135.
- (2) Hsu, J.-S.; Liang, B.-J.; Chen, S.-H. *Jpn. J. Appl. Phys.* **2005**, *44*, 6170–6173.
- (3) Dąbrowski, R.; Dziaduszek, J.; Ziółek, A.; Ł., Szczuciński, Stolarz, Z.; Sasnouski, G.; Bezborodov, V.; Lapanik, V.; Gauza, S.; Wu, S.-T. *Opto-Electron. Rev.* **2007**, *15*, 47–51.
- (4) Ziobro, D.; Dąbrowski, R.; Kula, P.; Dziaduszek, J.; Filipowicz, M.; Parka, J.; Czub, J.; Urban, S.; Wu, S.-T. *Opto-Electron. Rev.* **2009**, *17*, 16–19.
- (5) Weil, C.; Muller, S.; Scheele, P.; Best, P.; Lussem, G.; Jakoby, R. *Electron. Lett.* **2003**, *39*, 1732–1734.
- (6) Dąbrowski, R.; Dziaduszek, J.; Kula, P. US Pat. Application, No 61/112,771, 2008.
- (7) Dąbrowski, R.; Bezborodov, V.S.; Lapanik, V.J.; Dziaduszek, J.; Czupryński, K. *Liq. Cryst.* **1995**, *18*, 213–218.
- (8) Gestblom, B. In *Relaxation Phenomena*; Springer: Berlin, 2003.
- (9) HyperChemTM, Release 7.51, Hypercube, Inc., 2002; CS MOPAC ProTM, CambridgeSoft Corporation, 1996–1999.

- (10) Chełkowski, A. *Dielectric Physics*; Elsevier: Amsterdam, 1980.
- (11) Czub, J.; Gubernat, U.; Gestblom, B.; Dąbrowski, R.; Urban, S. *Z. Naturforsch.* **2004**, *59a*, 316–324.
- (12) Czub, J.; Urban, S.; Dąbrowski, R.; Gestblom, B. *Acta Phys. Polon. A* **2005**, *107*, 947–958.
- (13) Czub, J.; Dąbrowski, R.; Dziaduszek, J.; Urban, S. *Phase Trans.* **2009**, *82*, 485–495.
- (14) Marcelja, S. *J. Chem. Phys.* **1974**, *60*, 3599–3604.
- (15) Maier, W.; Meier, G.; *Z. Naturforsch.* **1961**, *16a*, 262–267.
- (16) Catalano, D.; Geppi, M.; Marini, A.; Veracini, C.A.; Urban, S.; Czub, J.; Kuczyński, W.; Dąbrowski, R. *J. Phys. Chem. C* **2007**, *111*, 5286–5299.
- (17) Geppi, M.; Marini, A.; Veracini, C.A.; Urban, S.; Czub, J.; Kuczyński, W.; Dąbrowski, R. *J. Phys. Chem. B* **2008**, *112*, 9663–9676.